

Crystallization of metal-oxide glasses in Bi-Sr-Ca-Cu-O systems

Donglu Shi, Ming Tang,* M. S. Boley,[†] Mark Hash,[‡] K. Vandervoort,[§]
H. Claus,[§] and Y. N. Lwin[†]

Materials Science Division, Argonne National Laboratory, Argonne, Illinois 60439

(Received 23 February 1989)

A crystallization study has been carried out for rapidly solidified Bi-Sr-Ca-Cu-O glasses with nominal compositions $\text{Bi}_2\text{Sr}_2\text{Ca}_2\text{Cu}_3\text{O}_x$, $\text{Bi}_2\text{Sr}_2\text{Ca}_3\text{Cu}_4\text{O}_x$, and $\text{Bi}_2\text{Sr}_2\text{Ca}_4\text{Cu}_5\text{O}_x$. A temperature-time-transformation diagram for the glass with nominal composition $\text{Bi}_2\text{Sr}_2\text{Ca}_2\text{Cu}_3\text{O}_x$ has been constructed, within which crystalline superconducting and nonsuperconducting phase regions are identified. Eutectic and primary crystallization have been found to occur during the annealing process in these metal oxides. Glass transition temperature T_g values, superconducting transition temperature values of crystallized products, and microstructural changes are measured and analyzed by differential thermal analysis, electrical resistivity, and magnetization shielding, x-ray diffraction, and scanning electron microscopy experiments. Also discussed are thermodynamics and kinetics of crystallization processes and the formation of the 110-K superconducting phase.

I. INTRODUCTION

The discovery^{1,2} of superconductivity in Bi-Sr-Ca-Cu-O systems has generated great interest in the fields of condensed matter physics and materials science. Since the first report from Michel *et al.*¹ research has been concentrated in the areas of crystal structure, phase diagrams, superconducting properties, and synthesis.³⁻⁶ The detailed structure work has revealed important information about the relationship between superconductivity and two-dimensional Cu-O planes in the orthorhombic unit cell. Investigations include extensive electron microscopy work in studying defects, intergrowth phenomena, and other microstructural characteristics of bismuth-based metal oxides.⁷⁻⁹ Various sample preparation techniques have also been developed to optimize the superconducting and other material properties of sintered products. Hinks *et al.* used a novel method to fabricate highly dense and homogeneous samples in a Bi-Sr-Ca-Cu-O system.¹⁰ Their method involved a rapid solidification technique by which samples were melted first and then splat quenched to form an amorphous structure. The crystalline phases were obtained through subsequent annealing of quenched glasses. The advantages of such a technique are threefold: (1) the products have an extremely dense matrix compared with ceramic-sintered samples; (2) since the samples are thoroughly melted, the chemical mixing is far more complete compared with the usual ball mill process; and (3) the microstructures of the crystallized material are highly controllable.

Since the amorphous structure is thermodynamically metastable, it crystallizes at elevated temperatures. The transition of the metastable amorphous structure into the crystalline phases can proceed by different reactions. If the amorphous structure crystallizes into just one phase without any concentration changes, it is called polymorphous crystallization. However, in many cases, crystallization occurs through complicated decomposition reac-

tions such as eutectic crystallization (i.e., simultaneous crystallization of several crystalline phases). These crystallization mechanisms result in various products with different physical properties and microstructures.

From the standpoint of material synthesis, the fabricated materials should possess properties such as phase purity, freedom from defects, high density, chemical stability, and controllable microstructures. These goals cannot be achieved until the crystallization, phase transformation, diffusion, and microstructures of the materials are fully understood. It is particularly important in bismuth-based superconductors that high-density single-phase samples with 110-K superconductivity can be routinely produced.

From a scientific standpoint, crystallization study of rapidly solidified glasses in Bi-Sr-Ca-Cu-O is of great interest. The nucleation and growth processes of both the 85-K and 110-K superconducting phases are not yet clear. The intergrowth of the 110-K phase has been observed, but the kinetics of this complicated process have not been thoroughly studied. It is difficult to study these mechanisms with ceramic-sintered samples since the microstructures are not easily controlled. In liquid-quenched oxide glasses, on the other hand, the starting material is a highly uniform and dense amorphous structure, and the crystallization can be carefully controlled by adjusting the annealing parameters. The whole phase change process can therefore be clearly observed by various characterization techniques.

We have investigated metal oxide glasses in Bi-Sr-Ca-Cu-O systems with nominal composition $\text{Bi}_2\text{Sr}_2\text{Ca}_2\text{Cu}_3\text{O}_x$ (2:2:2:3), $\text{Bi}_2\text{Sr}_2\text{Ca}_3\text{Cu}_4\text{O}_x$ (2:2:3:4), and $\text{Bi}_2\text{Sr}_2\text{Ca}_4\text{Cu}_5\text{O}_x$ (2:2:4:5). In particular, we have conducted annealing experiments over a wide temperature range (400–900 °C) for 2223 glass, with annealing times from 10 s to 16 d. Superconducting phases and microstructural changes during crystallization were analyzed by using x-ray diffraction (XRD), scanning electron microscopy (SEM), and differential thermal analysis (DTA). Superconducting properties were evaluated by electrical resistivity and

magnetization shielding experiments. In this paper we present the results of these analyses. We also discuss the thermodynamics and kinetics of crystallization and the formation of the 110-K phase.

II. EXPERIMENTAL PROCEDURE

Starting materials of Bi_2O_3 , SrCO_3 , CaCO_3 , and CuO were weighted in the atomic proportions of 2:2:2:3, 2:2:3:4, and 2:2:4:5. The weighed powders were thoroughly mixed by a wet ball mill in an agate container for 2–3 h. After ball milling, the mixed powders were dried and calcined in air at 800°C for 20 h. The calcined powders were melted in a platinum crucible and splat quenched between two copper blocks preheated at 200°C . Extremely dense glass sample plates with dimensions of $50 \times 40 \times 0.5 \text{ mm}^3$ were then formed for subsequent crystallization study. The 2223 glass samples were annealed at 400°C , 500°C , 600°C , 790°C , 850°C , 870°C , and 900°C for various times extending from 10 s to 16 d. The other two glasses 2234 and 2245 were annealed at 870°C for similar annealing time periods. All heat treatment experiments were done in air with heating and cooling rates of $27^\circ\text{C}/\text{min}$ and $7^\circ\text{C}/\text{min}$, respectively. Details about the same preparation technique can be found in Refs. 10–12.

X-ray diffraction data were taken by using a Rigaku diffractometer with $\text{Cu } K\alpha$ radiation. Electrical resistivity was measured by using a standard four-probe technique on annealed sample bars approximately $10 \times 1.7 \times 0.5 \text{ mm}^3$. The measuring current density used was $1.2 \text{ A}/\text{cm}^2$. Magnetization shielding data were taken using an SHE superconducting quantum interference device (SQUID) magnetometer in an applied field of 2 Oe from 10 to 150 K. The scanning electron microscope was a JEOL 840 A with a Tracor-Northern Model 5500 x-ray analysis system.

III. RESULTS

Figures 1–3 are x-ray diffraction plots for the 2223, 2234, and 2245 samples annealed at 870°C for different times. As can be seen in Fig. 1(b), eutectic crystallization occurs in the 2223 samples with eutectic products of 2212 and calcium- and copper-rich impurity Ca_2CuO_3 . The 85-K phase dominated as the annealing is extended to 5 d at 870°C and only a very small amount of Ca_2CuO_3 can be seen in Fig. 1(c) ($2\theta = 32^\circ$). However, the impurity level drastically increases as the calcium and copper concentrations are increased to nominal compositions 2234 and 2245. As shown in Fig. 2(a), large amounts of impurity phases (mostly Ca_2CuO_3 and CuO) have formed in the initially crystallized products. As crystallization proceeds, the 85-K phase subsequently precipitates from the amorphous matrix [Fig. 2(b)]. Significant amounts of the 110-K phase are formed until annealing at 870°C is prolonged to 7 d, showing that long-term diffusion is required for such a phase to nucleate and grow. The crystallization is complicated by a similar decomposition reaction as the calcium and copper contents are further increased to 2245 (Fig. 3). The 110-K phase reaches the maximum

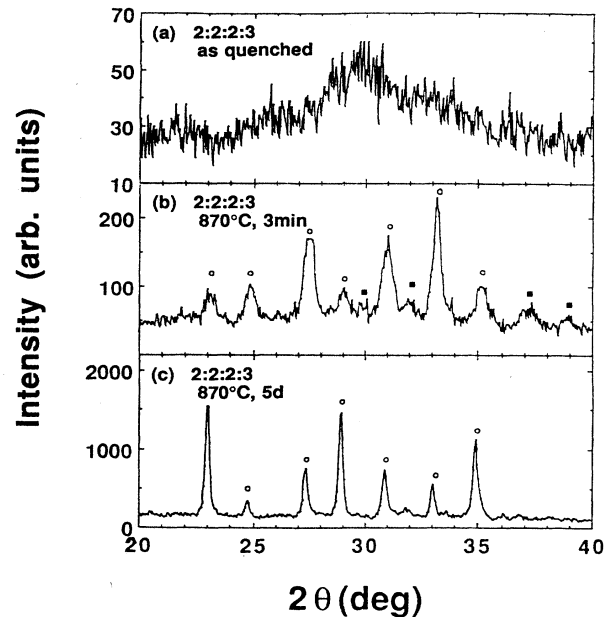


FIG. 1. X-ray diffraction plots for the 2223 samples (a) as quenched, (b) annealed at 870°C for 3 min, and (c) annealed at 870°C for 5 d. The symbol (○) is the 85-K phase and (■) for the Ca_2CuO_3 phase.

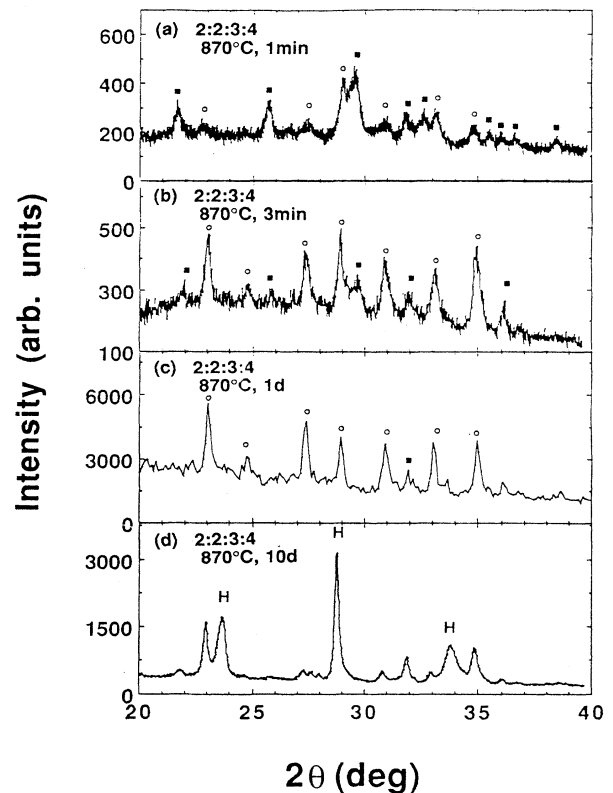


FIG. 2. X-ray diffraction plots for the 2234 samples annealed at 870°C for (a) 1 min, (b) 3 min, (c) 1 d, and (d) for 10 d. The symbol H is for the 110-K phase and (■) for the calcium- and copper-rich impurities such as Ca_2CuO_3 and CuO .

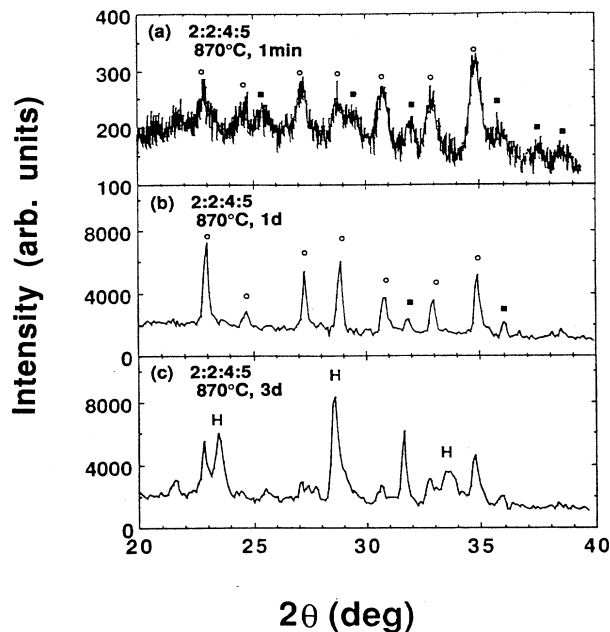


FIG. 3. X-ray diffraction plots for the 2245 samples annealed at 870°C for (a) 1 min, (b) 1 d, and (c) 3 d. The symbols are the same as used in Figs. 1 and 2.

amount as annealing proceeds to 3 d at 870°C [Fig. 3(c)]. This shows that the annealing time required for formation of the 110-K phase is much shorter compared with the 2234 samples.

In Fig. 4 we plot magnetization versus temperature for the 2223 glass samples annealed at 870°C for 1 min, 30 min, 1 h, and 4 h. As shown in the figure, the magnetization signal rapidly increases as annealing time increases from 1 min to 4 h. This indicates the increase of volume percent of 85 K with annealing time, and the time scale of crystallization. For the 2223 samples, we found that only very small amounts of the 110-K phase formed (less than 5%) as annealing at 870°C extended to 24 h (not shown).

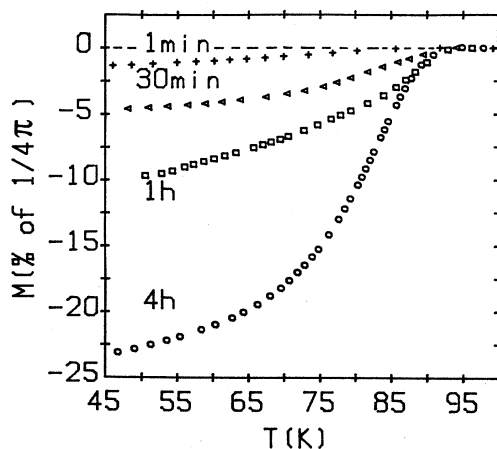


FIG. 4. Zero-field-cooled magnetization vs temperature for the 2223 samples annealed at 870°C for various times indicated in the figure.

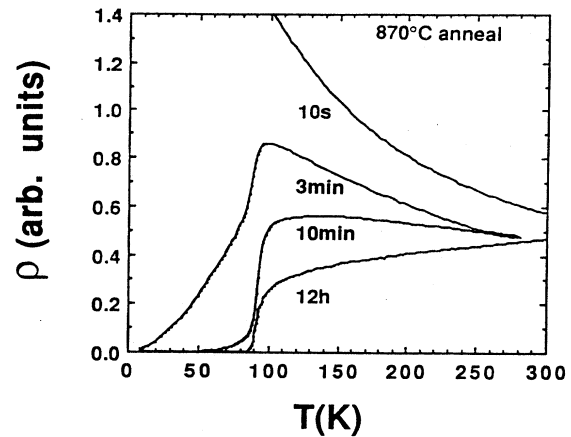


FIG. 5. Resistivity vs temperature for the 2223 samples annealed at 870°C for various times indicated in the figure.

In Fig. 5 we plot resistivity versus temperature for the 2223 glass sample annealed at 870°C for different times. As can be seen in the figure, the 10 s annealing did not result in significant crystallization, and the sample exhibits semiconducting behavior. At 3 min, the sample has partially crystallized, thus having a very broad transition. The superconducting transition thereafter sharpens near 85 K when annealing prolongs from 3 min to 12 h.

A single superconducting transition at 110 K has been observed in the crystallized 2234 and 2245 samples. As shown in Fig. 6(a), T_c ($\rho=0$) at 105 K has been obtained

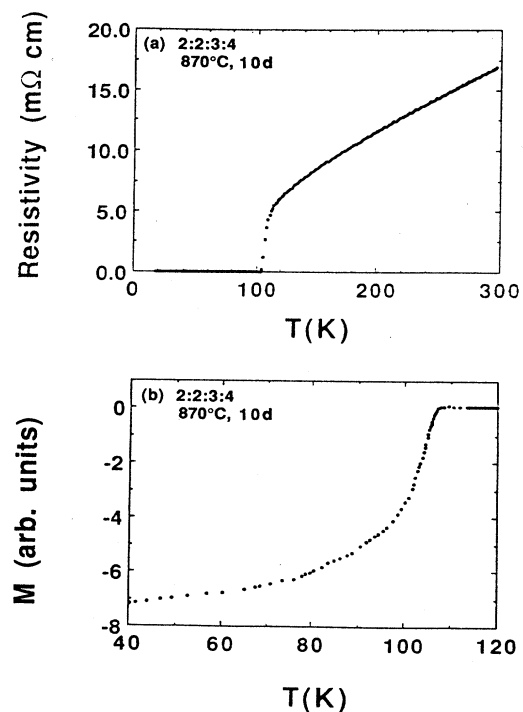


FIG. 6. (a) Resistivity vs temperature for the 2234 sample annealed at 870°C for 10 d; (b) zero-field-cooled magnetization vs temperature for the same sample shown in (a).

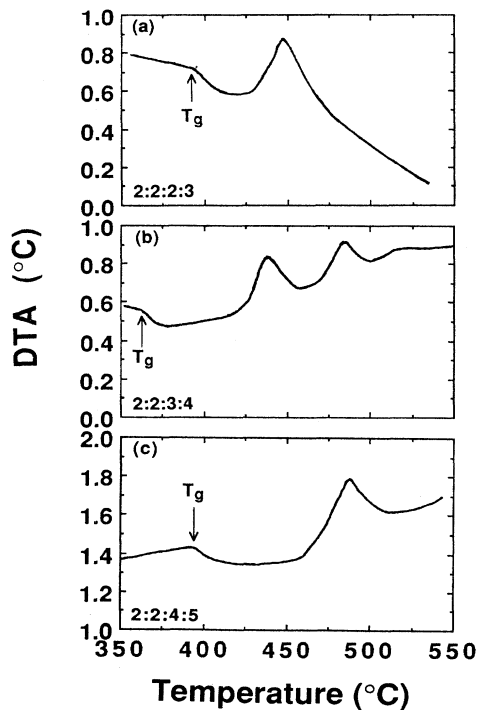


FIG. 7. DTA data for (a) the 2223 sample, (b) the 2234 sample, and (c) the 2245 sample. The heating rate used in the DTA experiment is 2°C/min.

in the 2234 samples annealed at 870°C for 10 d. The magnetization shielding data are shown in Fig. 6(b). It can be seen from the figure that the sample has a fairly sharp transition at 110 K; no transition at 85 K is found. Similar results are also obtained from the 2245 samples.

The glass transition temperatures T_g of 2223, 2234, and 2245 glasses have been obtained from DTA experiments as shown in Fig. 7. To emphasize the detailed features of the glass transition behavior, the melting events are not shown in the figure. As shown in Fig. 7(a), the glass transition temperature T_g of 2223 glass is around 393°C. The 2223 glass has been found to have

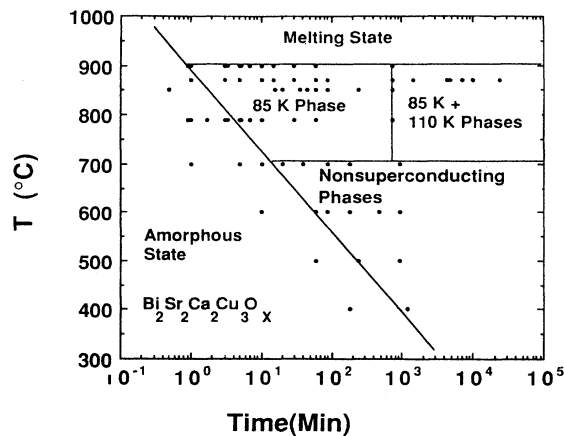


FIG. 8. The time-temperature-transformation diagram established for the 2223 samples based on the XRD, resistivity, and magnetization results.

three melting events. The major one occurs near 892°C. The 2234 glass has a glass transition temperature of 363°C. The 2234 glass has a relatively high melting point near 920°C. The glass transition temperature T_g of the 2245 glass is 406°C. The major melting event in the 2245 glass occurs at 980°C, which is the highest compared with that of the 2223 and 2234 glasses.

Using x-ray diffraction, electrical resistivity, and magnetization shielding data, we have constructed a time-temperature-transformation (TTT) diagram for crystallization of the 2223 samples shown in Fig. 8. Different phase regions are separated by solid lines, and every data point in the diagram is examined by both x-ray diffraction and resistivity measurements. The crystallization boundary (the boundary between the amorphous state and the crystalline phases) is for approximately 70% crystallization, determined from x-ray diffraction and

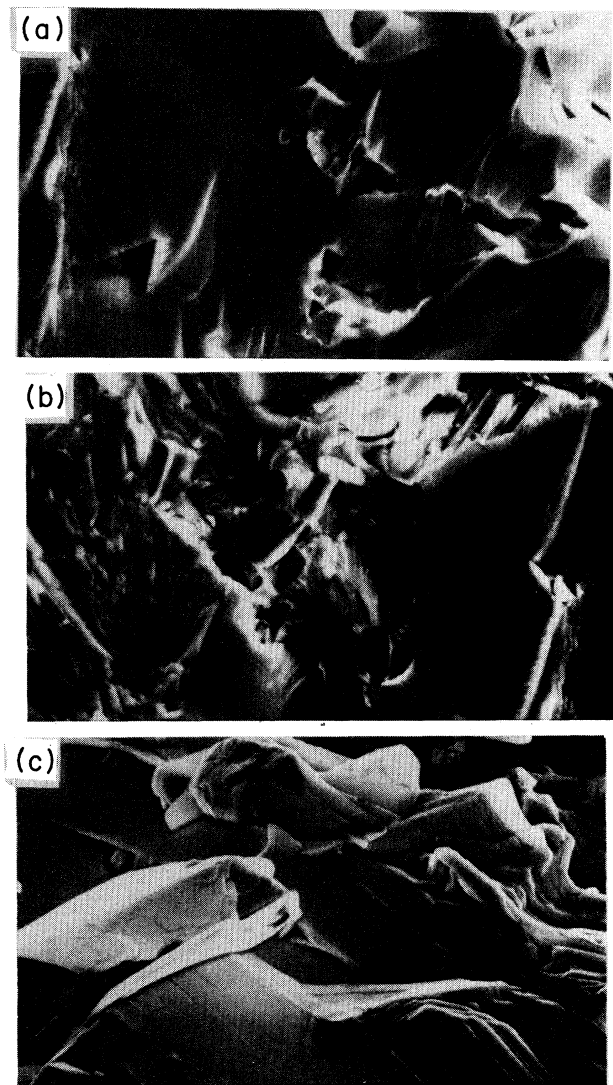


FIG. 9. Scanning electron microscopy photograph (secondary electron) of the 2223 samples annealed at 870°C for (a) 50 s, (b) 10 min, and (c) 4 h.

magnetization shielding data. As can be seen in the TTT diagram, crystallization takes place quickly (about 1 min) in the temperature range between 800°C and 900°C. However, the growth of the 110-K phase does not occur until an annealing time of 24 h is reached. As expected, it takes more than 1 h for the crystallization to begin near 500°C. Below 700°C most of the crystallized products are nonsuperconducting phases such as CuO, Ca₂CuO₃, and Bi₂O₃. None of the samples annealed in this temperature region is superconducting. Above 900°C, glass samples start to melt, which is consistent with the DTA data.

Some scanning electron microscopy results are shown in Fig. 9 for the 2223 samples annealed at 870°C for 50 s, 10 min, and 4 h. As can be seen in Fig. 9(a), annealing 50 s does not result in any significant crystallization. The matrix, therefore, is a uniform amorphous structure. Typical layered microstructures start to appear as the glass sample is heated at 870°C for 10 min [Fig. 9(b)]. However, there are still regions remaining with glass characteristics under this annealing condition. The highly layered microstructures are fully developed as annealing at 870°C prolongs to 4 h. As can be seen in Fig. 9(c), large platelike grains have formed typical in the Bi-Sr-Ca-Cu-O system; these grains are fairly well textured. It can also be seen from Fig. 9 that the crystallized samples possess a high matrix density compared with ceramic-sintered materials. This is one of the advantages of the technique reported in this paper.

IV. DISCUSSION

As indicated in the results section, the glass samples with all three nominal compositions 2223, 2234, and 2245 crystallize by eutectic reactions.¹³ The 2223 samples appear to have a nominal composition close to the eutectic point, judging from the relatively low melting temperature. The eutectic products are the 85 K phase and calcium- and copper-rich phases. The amounts of such phases increase as the calcium and copper concentration in the nominal composition is increased to 2234 and 2245. Some primary crystallization may occur before eutectic reaction takes place in the 2234 and 2245 glasses.

The whole crystallization process may be explained as follows: For the 2223 sample, there might not be any primary crystallization since it is near the eutectic point. The 85-K phase and impurity phases nucleate and grow together. As the 85-K phase (it has a composition of Bi₂Sr₂CaCu₂O_x) forms, the adjacent regions become rich in calcium and copper. Thus, calcium and copper are rejected from the 85-K phase and form their oxides on either side. Lamellae (sheets) of the two phases advance together into the unstable amorphous matrix. This process is schematically shown in Figs. 10(a) and 10(b).

Crystallization mechanisms of the 2234 and 2245 glasses may differ from that of the 2223 samples. These compositions should be further away from the eutectic point and thus have higher melting temperatures. When primary crystallization occurs, calcium- and copper-rich phases may precipitate first from the amorphous matrix. As more and more calcium- and copper-rich phases pre-

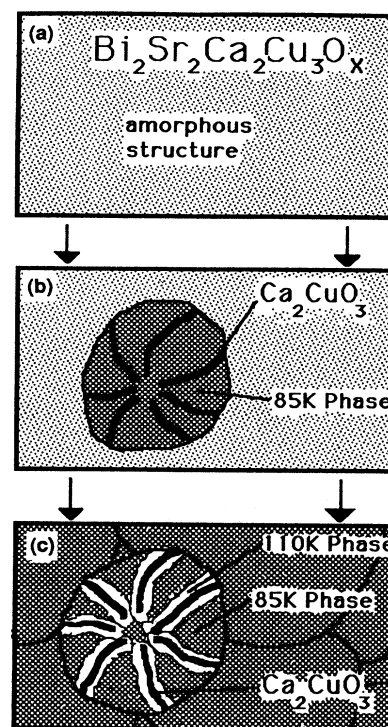


FIG. 10. Schematic diagrams for the crystallization mechanisms in 2223 glass and the formation of the 110-K phase: (a) amorphous matrix, (b) eutectic crystallization, and (c) formation of the 110-K superconducting phase.

cipitate, the composition of the adjacent amorphous phase will be shifted towards the eutectic point. The dispersed primary crystallized products may act as the preferred nucleation site for the subsequent crystallization. Eutectic crystallization will occur as the composition of the amorphous phase reaches the eutectic point. This eutectic reaction should be identical to that of 2223 glass (i.e., simultaneous crystallization of 85-K phase and calcium- and copper-rich phases).

An important fact observed in this crystallization study is that the 110-K superconducting phase does not crystallize directly from the amorphous phase.¹² It can form only as annealing is prolonged to at least 24 h at 870° for all nominal compositions investigated. We propose a microstructural model for the formation of the 110-K phase shown in Fig. 10(c). As stated above, eutectic crystallization occurs in the system, and interfaces between the 85-K phase and calcium copper oxide are therefore created, probably having the morphology shown in Fig. 10(b). Because of the high concentration difference in calcium and copper across the interface, diffusion of calcium and copper atoms towards the 85-K phase must occur at elevated temperatures. The 110-K phase (having a composition of Bi₂Sr₂Ca₂Cu₃O_x) will form at these interfaces after certain amounts of calcium and copper have diffused into the 85-K phase. The formation of the 110-K phase involves adding one more Ca-O and Cu-O planes in the 85-K phase unit-cell structure through so-called syntactic intergrowth. According to the classic nucleation theory¹⁴

$$I \propto n \nu \exp \left[\frac{-\Delta G_c}{KT} \right] \exp \left[\frac{-U}{KT} \right],$$

where I is the nucleation rate, n is the number of atoms per unit volume, ν is the oscillating frequency of the atoms, ΔG_c is the free energy required to form a nucleus of critical size r_c , U is the activation energy for an atom transporting across the interface of an embryo. The term $\exp(-\Delta G_c/KT)$ is associated with the driving force of nucleation, and the term $\exp(-U/KT)$ is related to the diffusion of the atoms. At high temperatures, atomic diffusivities are high and the largest contribution to nucleation comes from $\exp(-\Delta G_c/KT)$. ΔG_c determines the condition under which a crystallization process is possible, and is given as

$$\Delta G_c = \frac{16\pi\sigma^3 V_m^2}{3\Delta G^2},$$

where σ is the interfacial energy, V_m the molar volume, and ΔG the free-energy difference between the amorphous state and the crystalline phase, which is proportional to the amount of undercooling. Obviously, smaller ΔG_c is expected for greater value of ΔG , which implies lower free energy of the crystalline phase with respect to that of the amorphous phase. The 85-K phase has smaller unit cell c -axis value of 31 Å, thus having relatively lower free energy compared with the 110-K phase ($c=38$ Å). The free-energy increase of the 110-K phase is also associated with the insertion of one more Cu-O and Ca-O planes. This is the main explanation for the fact that the 85-K phase always crystallizes first from the amorphous matrix and the 110-K phase can form only after the sample has fully crystallized and the copper and calcium diffusion becomes significant at the interfaces.

As we have observed in this research, the diffusion process is obviously enhanced by increasing initial calcium and copper content. We have found that only very small amounts (less than 5%) of the 110-K phase can form in 2223 samples, indicating that the growth of the 110-K phase is limited by insignificant amounts of calcium and copper. The amounts of the 110-K phase rapidly increase as the calcium and copper level is increased to 2234 in the nominal composition [as indicated in Figs. 2(c) and 6(b)]. However, the time required for the 110-K phase to reach the maximum amount is 10 d at 870°C. This required time period is greatly shortened to 3 d at the same temperature as the calcium and copper contents are further increased to 2245, showing a highly advanced diffusion process. It has been widely reported that lead doping can greatly enhance the formation of the 110-K phase. However, the origin of such an enhancement has

never been clarified. Based on our experimental results, we suggest that the promotion of the 110-K phase is merely a result of lead's advancing the diffusion process during the heat treatment.

V. CONCLUSIONS

We have successfully formed a highly dense amorphous structure in Bi-Sr-Ca-Cu-O systems with nominal compositions 2223, 2234, and 2245. By subsequent annealing processes, we have reproducibly crystallized liquid-quenched glasses and obtained 110-K superconductivity (based on both resistivity and magnetization shielding experiments) with $T_c(\rho=0)$ at 105 K in annealed products. We have observed that eutectic crystallization occurs in all glasses investigated and that the eutectic products are 85 K plus calcium- and copper-rich phases. Using DTA and x-ray diffraction data, we conclude that the 2223 nominal composition should be close to a eutectic point, and 2234 and 2245 towards the calcium- and copper-rich phases in the phase diagram. We have constructed a TTT diagram for the crystallization of the 2223 glass according to which the superconducting phases form only in the temperature region between 700°C and 900°C. The 110-K phase does not directly crystallize from the amorphous matrix, and it nucleates and grows only at the interfaces between eutectic products controlled by calcium and copper diffusion. The intergrowth process in the 85-K phase unit cell is accomplished by calcium and copper atoms diffusing across such an interface. The annealing time required for the maximum 110-K phase to form depends on the calcium and copper level in the nominal composition. For 2234 and 2245, the time is 10 d and 3 d, respectively, indicating that the diffusion processes are greatly enhanced by higher contents of calcium and copper. For the 2223 glass, only 5% of the 110-K phase can form in crystallized samples.

ACKNOWLEDGMENTS

We are grateful to Richard Lee for performing the scanning electron microscopy experiment. We are also grateful to Shiyou Pei for his valuable suggestions and discussions. This research is supported by the U.S. Department of Energy, Basic Energy Sciences—Materials Sciences, under Contract No. W-31-109-ENG-38. One of the authors (M.T.) is also supported by the National Science Foundation and the Wisconsin Alumni Research Fund, and thanks are given to Dr. Marshall Onellion for useful conversations.

*Present address: Materials Science Program and Synchrotron Radiation Center, University of Wisconsin, Madison, WI 53706.

†Permanent address: Department of Physics, Western Illinois University, Macomb, IL 61455.

‡Permanent address: Chemical Technology Division, Argonne National Laboratory, Argonne, IL 60439.

§Permanent address: Department of Physics, University of Illinois at Chicago, Chicago, IL 60680.

¹C. Michel, M. Herrien, M. M. Borel, A. Grandin, F.

- ²H. Maeda, Y. Tanaka, M. Fukutomi, and T. Asano, *Jpn. J. Appl. Phys. Lett.* **27**, L209 (1988).
- ³S. S. Parkin, V. Y. Lee, A. I. Nazzal, R. Savoy, R. Beyers, and S. J. LaPlace, *Phys. Rev. Lett.* **61**, 750 (1988).
- ⁴R. M. Hazen, C. T. Prewitt, R. J. Angel, N. L. Ross, L. W. Finger, C. G. Hadriacos, D. R. Veblen, P. J. Heany, P. H. Hor, R. L. Meng, Y. Y. Sun, Y. Q. Wang, Y. Y. Xue, Z. J. Huang, L. Gao, J. Bechtold, and C. W. Chu, *Phys. Rev. Lett.* **60**, 1174 (1988).
- ⁵M. A. Subramanian, C. C. Torardi, J. C. Calabrese, J. Gopalakrishnan, K. J. Morrissey, T. R. Askew, R. B. Flippen, U. Chowdhry, and A. W. Sleight, *Science* **239**, 1015 (1988).
- ⁶S. A. Sunshine, T. Siegrist, L. F. Schneidmeyer, D. W. Murphy, R. J. Cava, B. Batlogg, R. B. van Dover, R. M. Flemming, S. H. Glarum, S. Nakahara, R. Farrow, J. J. Krajewski, S. M. Zahurak, J. V. Waszczak, J. H. Marshall, P. Marsh, L. W. Rupp, Jr., and W. F. Peck, *Phys. Rev. B* **38**, 893 (1988).
- ⁷H. W. Zandbergen, Y. K. Huang, M. J. V. Menken, J. N. Li, K. Kadowaki, A. A. Menovsky, G. Van Tendeloo, and S. Amelinckx, *Nature* **333**, 620 (1988).
- ⁸H. W. Zandbergen, P. Goren, G. Van Tendeloo, J. Van Landuyt, and S. Amelinckx, *Solid State Commun.* **66**, 397 (1988).
- ⁹I. K. Schuller and J. D. Jorgensen, *MRS Bull.* **XIV**(1), 27 (1989).
- ¹⁰D. G. Hinks, L. Soderholm, D. W. Capone II, B. Dabrowski, A. W. Mitchell, and D. Shi, *Appl. Phys. Lett.* **53**, 423 (1988).
- ¹¹D. Shi, M. Blank, M. Patel, D. G. Hinks, and A. W. Mitchell, *Physica C* **156**, 822 (1988).
- ¹²Donglu Shi, Ming Tang, K. Vandervoort, and H. Claus, *Phys. Rev. B* **39**, 9091 (1989).
- ¹³U. Koster and U. Herold, in *Glassy Metals I*, Vol. 46 of *Topics in Applied Physics*, edited by H. J. Gunterodt and H. Beck (Springer-Verlag, New York, 1981).
- ¹⁴H. Rawson, *Inorganic Glass-Forming Systems* (Academic, London, 1967).
- ¹⁵J. W. Cahn and R. J. Charles, *Phys. Chem. Glasses* **6**(5), 181 (1965).

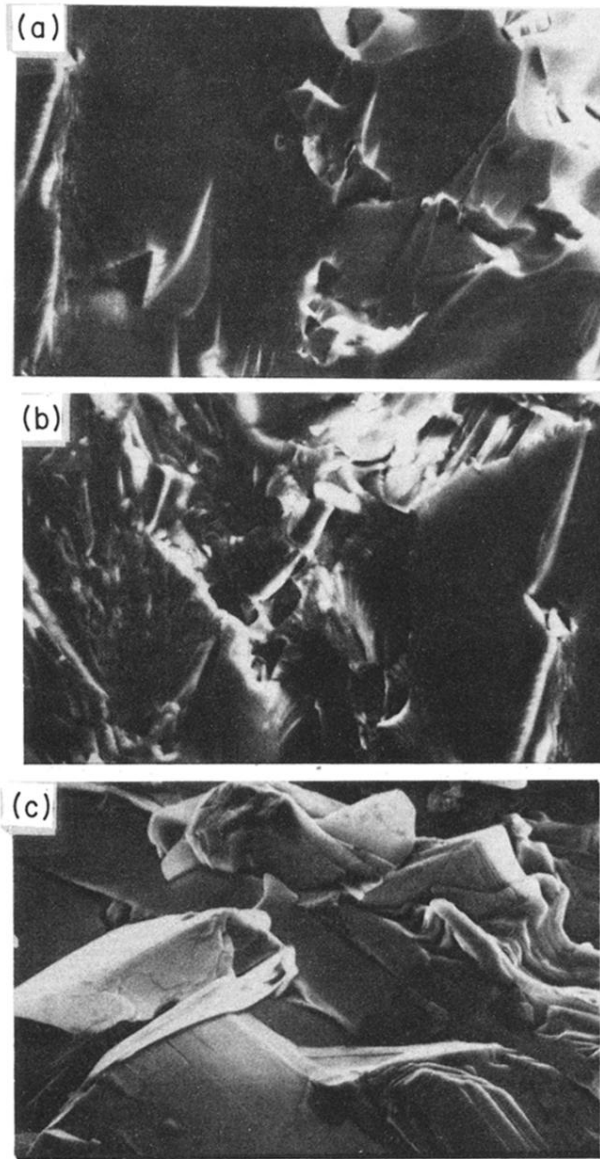


FIG. 9. Scanning electron microscopy photograph (secondary electron) of the 2223 samples annealed at 870 °C for (a) 50 s, (b) 10 min, and (c) 4 h.